Analytical Methods

PAPER

Analytical Methods Accepted Manuscript

Mapping the resting and stimulated EGFR in cell membranes with topography and recognition imaging

Weidong Zhao[#,a,b], Yangang Pan[#,a,b], Jiazhen Wu[a], Mingjun Cai[a], Yongmei Tian[a], Haijiao Xu[a], Lihua Yu[c] and Hongda Wang[*a,b]

Epidermal growth factor receptor (EGFR) is widely spread in various types of cells and plays critical roles in cellular activities. Here we studied the EGFR distribution before and
10 **after activation by high resolution mapping technique-topography and recognition imaging (TREC). The unbinding force between EGFR and its ligand, epidermal growth factor (EGF), was also measured by single-molecule force spectroscopy. Our results suggest that the majority of EGFRs**
15 **are in the cluster state both in the resting and stimulated cells. This study provides the qualitative information of the location, cluster state and binding kinetics of EGFRs in cell membranes at the molecular level.**

Introduction

20 EGFR (also known as ErbB1 or HER1), one of the most important and best studied receptors, belongs to the ErbB receptor family that can mediate the intracellular signaling pathways of growth factors, such as EGF[1]. EGFR is widely distributed in epithelial and stromal cells, and several types of
25 smooth muscle and glial cells[2]. EGFR is a transmembrane protein as depicted in Fig. 1A. After binding EGF, EGFR can dimerize, which will induce the activation of tyrosine kinase domains and deeper cellular activities[3]. Its signaling pathways can activate mitogenesis signaling, cell apoptosis, protein secretion, cell
30 migration[4], and it is also involved in organ morphogenesis, repair and maintenance[2]. More importantly, EGFR and EGF levels are usually found to be overexpressed in many types of human tumors, for instance, the lung cancer and breast cancer[5]. The autocrine pathway of EGFR can contribute to cancer cell
35 proliferation, angiogenesis and apoptosis. Thus it is supposed to be extensively relevant in tumor development, metastasis and invasion, and is regarded as the target in cancer therapy[6].

40 *[a] State Key Laboratory of Electroanalytical Chemistry, Changchun Institute of Applied Chemistry, Chinese Academy of Sciences, Changchun, Jilin 130022, P.R. China.*
[b] University of Chinese Academy of Sciences, Beijing 100049, P.R. China.
[c] School of Life Sciences, Chongqing University, Chongqing 400030, P.R.
45 *China.*
[#] These authors contributed equally.
* Corresponding author:hdwang@ciac.ac.cn

As the receptor location and binding kinetics between the receptors and the corresponding signal molecules keep key roles
50 in cell adhesion, differentiation, and so on[7], many studies attempt to localize EGFR in cells[8,9]. Distributions of ErbB receptors on membranes of SKBR3 breast cancer cells were mapped by immunoelectron microscopy[10]. Single particle tracking have been used for exploring the dynamics of EGFR in the membrane[11,12].
55 Near field scanning optical microscopy (NSOM) by Abulrob et al. suggested that EGFR might form clusters in fixed Hela cells[13]; Gadella et al. detected EGF receptor dimerization and its conformational state by Fluorescence resonance energy transfer (FRET)[14]; Schlessinger et al. measured the kinetics of EGF
60 binding to soluble EGF receptor by surface plasmon resonance[15]. However, the localization of EGFRs in original and activated states in cell membranes at single molecular level has not been achieved yet, meanwhile the binding affinity and kinetics between EGFR-EGF at single molecule level on intact cells are
65 still unclear.

Atomic Force Microscopy (AFM) has achieved great success in many fields since it was invented in 1986[16]. AFM can image the biological samples at the sub-nanometer level both in air and in solution[17-20]. Single-molecule force spectroscopy is a powerful
70 toolkit to study the force at the piconewton level because of the high sensitivity of the AFM and the use of soft cantilevers[21]. With force spectroscopy, the binding kinetics of antigen-antibody, biotin-avidin, receptor-ligand and other systems have been investigated[22,23,24]. The topography and recognition imaging
75 (TREC), the combination of AFM imaging and single-molecule force spectroscopy, has extended the ability of AFM to localize specific molecules in the heterogeneous samples[25]. TREC can image the biological samples with functionalized (i.e. antibody or ligand) AFM tips and a recognition image is generated
80 simultaneously, which can accurately recognize and position the corresponding target molecules (such as antigen or receptor) with high lateral accuracy (at single molecular resolution) under native conditions. It has been affirmed to be efficient in the recognization of the chromatins, membrane proteins and other
85 molecules of cells[26-28].

In this work, we directly studied the location and cluster states of the resting and stimulated EGFRs on cell surfaces by TREC, and investigated the interaction forces between EGFR and EGF

on live cells by force spectroscopy. These studies provide insights to the activation process of EGFR at the nanoscale level.

Materials and Methods

Cell culture

A549 Cells were cultured on glass cover slides in Dulbecco's modified Eagle's medium (DMEM, Hyclone) supplemented with 10% heat inactivate fetal bovine serum (Hyclone), 100 U/mL penicillin, 100 μg/mL streptomycin and 50 μg/mL blasticidin S (InvivoGen). Cells were grown at 37 °C in a humidified atmosphere with 5% CO_2. Usually, it requires one or two days for the cells to achieve a uniform monolayer on the glass slides.

Modification of the AFM tips with EGF or antibody

Modification of the tips with EGF or antibody was performed as described[23]. Briefly, the tips were cleaned at O_3 atmosphere in UV-cleaner for 20 min to get rid of the organic contamination. Then the tips were vapor treated with aminopropyltriethoxysilane (APTES), and reacted with PEG crosslinkers in triethylamine (Sigma) and $CHCl_3$. Then the cantilevers were immersed in 100 μg/mL EGF (Rocky Hill, NJ) or rabbit anti-human EGFR (1005) antibody (EGFR (1005) is available as either rabbit (sc-03) or goat (sc-03-G) polyclonal affinity purified antibody raised against a peptide mapping at the C-terminus of EGFR of human origin. Groundwork biotechnology diagnosticate) solutions with $NaCNBH_3$ as catalyst. In the last, 1 M ethanolamine was added to passivate the unreacted aldehyde groups. Then the modified tips were rinsed with 150mM phosphate buffered solution (PBS, pH 7.5) for two times and stored in PBS at 4 °C until use.

Atomic force microscopy

All the AFM experiments were performed by the AFM 5500 (Agilent Technologies, Chandler, AZ). All the tips were purchased from Veeco (Microlevers, Veeco Metrology LLC, Santa Barbara, CA). The size and height of the cells and the recognition signals were measured with the PicoScan 5.3.3 software (Agilent Technologies, Chandler, AZ). The topography and amplitude images of the cells were acquired by the Acoustic AC (AAC) mode AFM at room temperature in DMEM with bare silicon nitride tips with spring constants of 0.01 N/m (nominal). The images were acquired as 512 × 512 pixels at scan rates of 1.7 Hz.

TREC was carried out with the silicon nitride cantilever tips with spring constants of 0.05 N/m (nominal) that were modified with EGF or antibody as described above. TREC was performed by Magnetic AC (MAC) Mode with PicoTREC imaging accessory (Agilent Technologies, Chandler, AZ) in buffer solution at room temperature. The recognition images were acquired as 512 × 512 pixels with scan rates of 1 Hz. In the study of the resting state of EGFR, the cells were fixed with 4% paraformaldehyde, and then were rinsed with PBS for three times. Blocking experiments were performed by the addition of 1 mg/mL EGF to the AFM sample cell. In the investigation of the stimulated state of the EGFR, the cells were stimulated with 3 μg/mL EGF on ice for 5 min, then were washed with PBS for three times. The blocking experiments were carried out by the injection of anti-EGFR antibody for 1 h.

Force spectroscopy was performed by force-distance mode in DMEM at 37 °C with EGF modified silicon nitride tips of 0.03 N/m spring constant (nominal). The blocking experiments were carried out with the addition of 1 mg/mL EGF to the sample chamber. Several thousand force curves were recorded at different positions on the cells. The deflection sensitivity of the photo-detector was determined by the slope of the force-distance curves taken on the newly cleaved bare surface of mica. The spring constants of the AFM cantilevers were measured with the thermal noise method in air by AFM multimode 8 (Veeco Metrology LLC, Santa Barbara, CA)[29]. The data of the force curves were processed with MatLab 7.9 (Math Works Inc.)

Fluorescence microscopy

A549 cells in which the EGFR was stably transfected by GFP were a generous gift from Prof. Xiaohong Fang (Institute of Chemistry, Chinese Academy of Sciences). Fluorescence microscopy imaging was performed by total internal reflection fluorescence microscopy (TIRFM). Cells were washed by 150 mM PBS for three times to remove the DMEM before imaging. GFP was excited with the 473 nm laser line. All the images were acquired on a 100×/1.4 oil-immersion objective.

Results

The surface morphology of A549 cells

Human lung adenocarcinoma cell line A549, due to the high expression of EGFR, was chosen to investigate the location of EGFRs and the binding kinetics between EGFR and EGF. The image of the bottom membrane of an entire A549 cell in which EGFRs were stably transfected with green fluorescent proteins was acquired with total internal reflection fluorescence microscopy (TIRFM). The image shows that an abundance of EGFR was expressed in cell membranes, as shown in Figure 1B. To observe the state of live cells, they were imaged by AFM in native conditions. The topography and corresponding amplitude images on cellular monolayer were shown in Fig. 1C and 1D, respectively. The images were acquired by Acoustic AC (AAC)
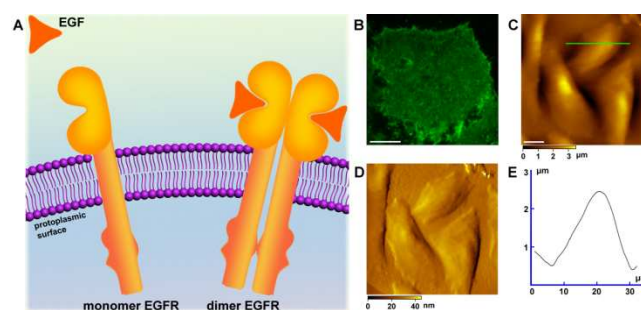
Fig. 1 The scheme of the structure of EGFR and the surface morphology of A549 cells. (A) EGFR is a transmembrane protein. There is the resting monomer (left). Upon binding with EGF, they can dimerize (right); (B) the TIRFM image of one GFP transfected cell; (C) and (D) the topography and corresponding amplitude images of A549 cells, respectively; (E) the cross section analysis along the green line in (C). Scale bars: 10 μm in (B) and (C)

mode, which can cause minimum damages on the morphology and activity of the biological samples[27]. The cells, with the diameter of 20-40 μm, were distributed healthily on the cover slides. The bright areas in Fig. 1C correspond to the nuclear region with the height of about 2 μm as shown in Fig. 1E. The cells were attached firmly on the glass cover slides and can be kept alive for 4 hours at room temperature, which are suitable for the molecular recognition imaging and force spectroscopy experiments.

Detection of EGFR in the resting state

As the resolution of fluorescence microscopy is limited, we employed TREC to detect and localize EGFR in cell membranes at single molecular resolution. The AFM tip was functionalized with EGF via the heterobifunctional aldehyde-PEG (polyethylene glycol)-NHS crosslinker as shown in the left of Fig. 2A. The PEG crosslinker (about 10 nm in length) was attached onto the tip by the NHS ester terminus and the amino groups on the APTES modified tip. The flexible PEG makes the tip-bound molecules to easily recognize the target receptors in the samples. The cells were scanned with magnetically coated probes by Magnetic AC (MAC) mode as depicted in the right part of Fig. 2A. In this mode, the tip is oscillated by the magnetic force during imaging, which can largely reduce the distortion to samples. When the EGFR sites were scanned with the EGF modified tips, the crosslinker will be stretched in the retraction process of the cantilever. The resulting energy loss will reduce the top peak of the oscillations; thus the recognition signal can be achieved and detected. The raw deflection signal of the cantilever is split by the TREC box, and the lower (minima) and upper (maxima) parts of each sinusoidal oscillating period were recorded as the topography and recognition images, respectively (as depicted in Fig. 2B). When the EGF bound EGFR sites during the scanning process, the interaction of EGF/EGFR would not be likely ruptured during tip oscillating (about 15 oscillations/pixel in our experiment), which is the reason that we obtain the recognition signal. Until the distance between AFM tip and EGFR became more than the length of PEG linker during the scanning process, the EGF/EGFR complex would be separated. As a result, the max size of recognition spot for single EGFR could be the double size of PEG linker (~20nm). Although the AFM tip can probably detect one EGFR multiple times during TREC process, it will not affect the size of the recognition spots. The recognition efficiency (more than 90%) has been tested [25], and single molecule detection can be achieved[30].

Fig. 2C shows the topography of the cell membrane. The dark dots in Fig. 2E display the recognition signals, which indicate the nonuniform distribution of EGFR domains in membranes. In order to clearly demonstrate the distribution of EGFR, the recognition signal was superimposed onto the topography image as shown in Fig. 2D (the green areas). The recognition signals correspond to part of high features in Figure 2c, indicating that these features may include EGFR. To verify the specificity of the recognition events, blocking experiment was performed by the addition of 100 μg/mL EGF into the sample chamber for 1 h. As the binding sites of EGFR were occupied with free EGF, the recognition signals disappeared as shown in Fig. 2F. A magnified recognition site was shown in Fig. 2G. The amplitude reduction

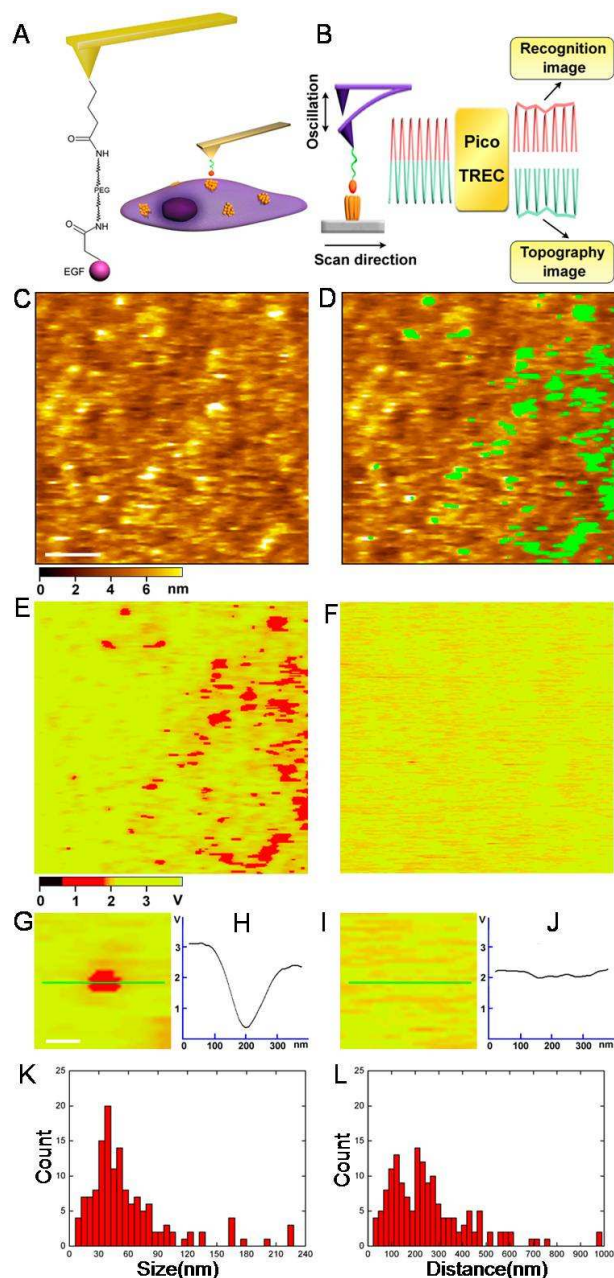of the cantilever was about 2.7 V according to the cross section

Fig. 2 The molecular recognition images of EGFR in the resting state on the cell surface. (A) the schematic of the AFM tip modified with EGF by the heterobifunctional PEG crosslinker (left part); the cell surface was scanned with the functionalized AFM tip (right part); (B) the principle of TREC; (C) and (E) the topography and the corresponding recognition images captured with EGF modified tips, respectively; (D) the topography with the recognition signal superimposed (shown as the green dots); (F) the recognition image after blocking by free EGF; (G) and (I) the magnified images from (E) and (F), respectively; (H) and (J) the cross section analysis along the green lines in (G) and (I), respectively; (K) the size distribution of the recognition signals from multiple areas in different cells; (L) the distance distribution of the adjacent recognition signals from multiple areas in different cells. Scale bars: 500 nm in (C), (D), (E) and (F); 100 nm in (G) and (J).

analysis depicted in Fig. 2H. The corresponding blocked area is shown in Fig. 2I, indicating that the recognition site was efficiently blocked as depicted in Fig. 2J (about 0.3 V). The size distribution of the EGFR recognition signals is shown in Fig. 2K. The sizes of most recognition spots are more than 20nm. The distance distribution of the adjacent EGFRs varies from 30 nm to 980 nm as shown in Fig. 2L. Therefore, we could speculate that most EGFRs in the resting state exist in the cluster form but not as single monomer, which is consistent with the results from direct stochastic optical reconstruction microscopy (dSTORM)[31]. This type of EGFR distribution may make it to be easy to form the dimer when activated, which is suitable for the cells to respond quickly to ligand-induced changes.

Detection of EGFR in the stimulated state

After the EGFR was stimulated with EGF, the signal pathways can be activated and further cellular activities will be induced. To locate the activated EGFR, cells were stimulated with EGF as described previously and then scanned by TREC[32]. As the ligand binding sites of EGFR were occupied with EGF, we located the EGFR with anti-EGFR antibody that binds different sites from
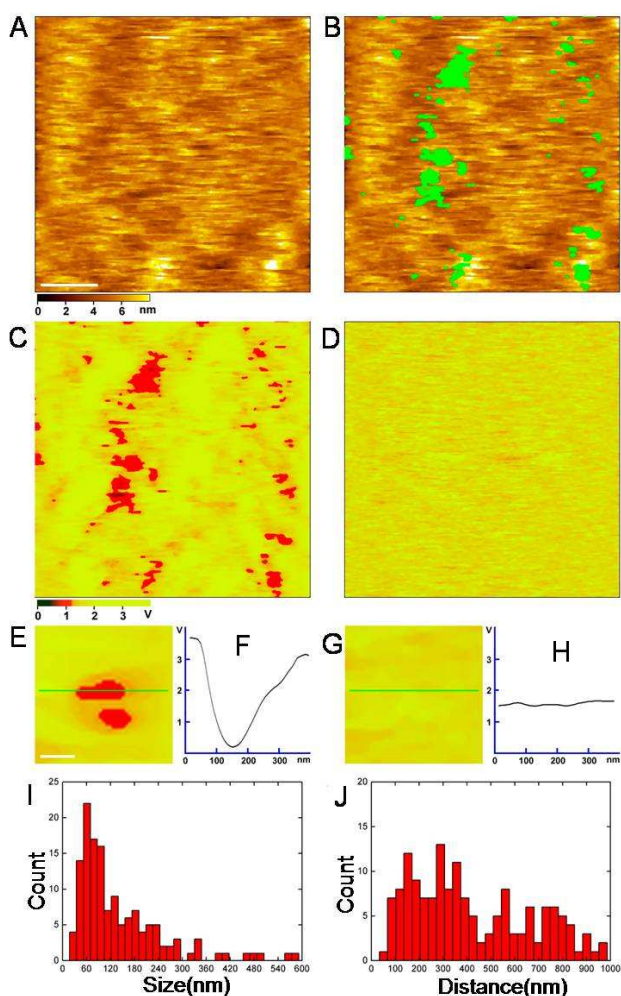

Fig. 3 The molecular recognition image of EGFR in the stimulated state on the cell surface. (A) and (C) the topography and the corresponding recognition images acquired with anti-EGFR antibody modified tips after the cells were stimulated with EGF; (B) the topography images with the recognition spots superimposed in it (shown as the green areas); (D) the recognition images after blocking with free antibody; (E) and (G) the magnified images from (C) and (D), respectively; (F) and (H) the cross section analysis along the green lines in (E) and (G), respectively; (I) the size distribution of the recognition sites in (C); (J) the distribution of the distances of the adjacent recognition sites in (C). Scale bars: 500 nm in (A), (B), (C) and (D); 100 nm in (E) and (G).

EGF. And the binding specificity between the antibody and receptors has been confirmed by immunocytochemical staining and molecular recognition imaging[7]. Fig. 3A and 3C shows the topography and recognition images of the stimulated cell membranes scanned with antibody conjugated tips, respectively. The recognition signal was superimposed onto the topography as depicted in Fig. 3B and the proteins (brightened dots) correspond well with the recognition areas. The reduction of the amplitude of the AFM cantilever in the recognition events was about 3.5 V (as shown in Fig. 3F). After the blocking experiments were carried out by the addition of free antibody, the recognition signals disappeared as shown in Fig. 3D. And the amplitude reduction dramatically decreased to about 0.2 V as shown in Fig. 3H, which reveals that the recognition event has been efficiently blocked.

The distributions of sizes and distances of adjacent recognition spots are depicted in Fig. 3I and 3J, respectively. The recognition spots with the sizes ranging from 35 nm to 105 nm take a percentage of 49%. There are also large areas that are about 600 nm in size. The distances of adjacent recognition areas are mainly in the range of 100-350 nm, which take a percentage of 35%. The sizes and distances of recognition areas are only slightly larger than that in the resting state. These results reveal that the EGFRs exist in cluster and close to each other in the resting state, in which they form the domains. This phenomenon could be important for the rapid dimerization while EGFRs are activated.

Detection of the interaction force between EGF and EGFR

To reveal the dynamics of the interactions between EGFR and EGF, AFM force spectroscopy were engaged as shown in Fig. 2A. In force-distance mode, the tip moves towards and withdraws from the cell monolayer as depicted in the right part of Fig. 2A. The deflection of the cantilever during the approach and retraction processes was recorded as the force-distance cycles. The specific interactions of the EGFR and EGF were characterized with the distinct unbinding force (in the retraction cycle). Because of the stochastic nature of the binding events, it is not possible to detect the individual EGFR on the surface every time; thus thousands of force curves were acquired at different locations on multiple cells. The typical force curve with single unbinding event is shown in Fig. 4A, which confirms the existence of EGFR on the cell surface. The distribution of the unbinding forces is depicted in Fig. 4C, and the values range from 12-89 pN with the maximum distribution at 36 ± 15 pN at a loading rate of 1.3×10^3 pN s^{-1}. Our results are similar to the unbinding forces of anti-VEGFR2/VEGFR2 (a similar receptor to EGFR)[7]. The overall binding probability is 14.7%. After the block experiment was carried out by the injection of EGF into the AFM sample cell for 1 h, the specific unbinding events disappeared in the force curve as shown in Fig. 4B since the binding sites of the EGFR were occupied. The binding

probability significantly decreased to 3.6% (as shown in Fig. 4D). There are no unbinding events in the force curves when the experiments were performed by the bare or PEG modified tips (as depicted in Fig. 4E). These results indicate that EGFR in cell membranes has been detected specifically and efficiently at the single molecular level.

The unbinding force of the receptor-ligand not only depends on the molecules themselves, but also depends on the loading rate of the tip[33]. The relation of unbinding force and loading rate follows the equation (1) as stated by the single barrier model:

$$f_u = \frac{k_B T}{x_\beta} \ln(\frac{r x_\beta}{k_B T k_{off}})$$

where f_u is the most probable unbinding force; x_β is the separation energy barrier from the equilibrium position; r is the loading rate, $r = k_{eff}v$, k_{eff} is the effective spring constant of the cantilever, v is the retraction velocity; k_{off} is the thermal off rate constant for dissociation at zero force; T is the thermodynamic temperature (in this experiment T = 310.15 K); k_B is the Boltzmann constant[33].

The corresponding unbinding forces were recorded with different loading rates. The relation between f_u versus lnr is depicted in Fig. 4F. From the fitting curve it can be known that f_u linearly correlates with lnr, which coincides well with the situation for a single barrier. It can be calculated $x_\beta = 0.16$ nm, $k_{off} = 9.1 \times 10^{-3}$ s^{-1}, which agrees well with that obtained in other receptor-ligand systems[35,36], demonstrating that the EGFR-EGF complex is much stable, which is essential in their signaling pathways. Therefore we directly reveal the bind affinities, kinetics and the energy landscape of EGFR and EGF on single molecular and individual cellular level.
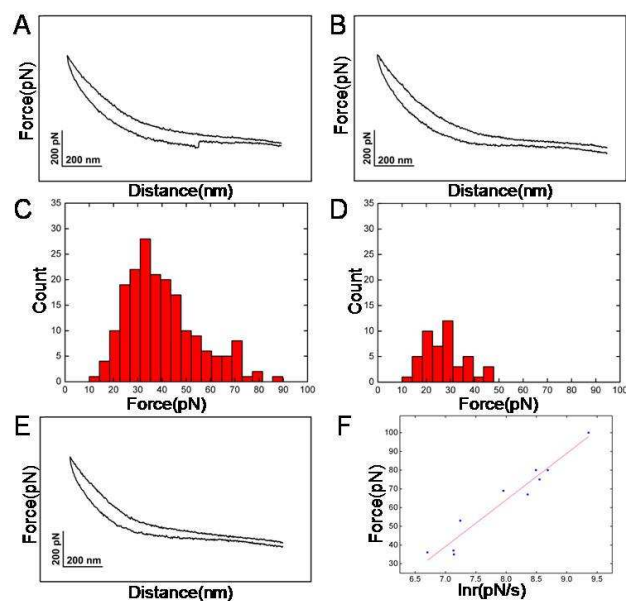

Fig. 4 The force spectroscopy of the interaction of EGFR-EGF. (A) the typical force curve shows the unbinding event; (B) the typical force curve after blocking with 1 mg/mL EGF, the unbinding event has disappeared; (C) and (D) the histograms of the unbinding forces before and after blocking; (E) the force curves of control experiments performed with bare tips or PEG modified tips; (F) the curve of the unbinding forces (pN) versus the natural logarithm of the loading rates (pN s^{-1})

Conclusions

In summary, we localized EGFR both at the resting and the stimulated states in cell membranes by TREC at single molecular resolution, which reveals that EGFR tended to form clusters and nonuniformly distributed in cell membranes. In the resting state, the majority of EGFRs existed in clusters rather than as isolated single proteins. There was no significant disparity in the sizes and distances between the resting and stimulated states. In addition, we directly revealed the bind affinities, kinetics and the energy landscape of EGFR/EGF. Our results may provide the new insights in the distribution of EGFR in cell membranes and its mechanism of activation,

References

1. R. N. Jorissen, F. Walker, N. Pouliot, T. P. J. Garrett, C. W. Ward and A. W. Burgess, *Exp. Cell Res.*, 2003, **284**, 31-53.
2. A. Wells, *Int J. Biochem. Cell Biol.*, 1999, **31**, 637-643.
3. M. A. Olayioye, R. M. Neve, H. A. Lane and N. E. Hynes, *EMBO J.*, 2000, **19**, 3159-3167.
4. R. S. Herbst, *Int. J. Radiat. Oncol. Biol. Phys.*, 2004, **59**, 21-26.
5. F. Ciardiello and G. Tortora, *Clin. Cancer Res.*, 2001, **7**, 2958-2970.
6. E. S. Kim, F. R. Khuri and R. S. Herbst, *Curr. Opin. Oncol.*, 2001, **13**, 506-513.
7. S. Lee, J. Mandic and K. J. Van Vliet, *Proc. Natl. Acad. Sci. U. S. A.*, 2007, **104**, 9609-9614.
8. K. Roepstorff, P. Thomsen, K. Sandvig and B. van Deurs, *J. Biol. Chem.*, 2002, **277**, 18954-18960.
9. S. V. Matveev and E. J. Smart, *Am. J. Physiol.-Cell Physiol.*, 2002, **282**, C935-C946.
10 S. Yang, M. A. Raymond-Stintz, W. Ying, J. Zhang, D. S. Lidke, S. L. Steinberg, L. Williams, J. M. Oliver and B. S. Wilson, *J. Cell Sci.*, 2007, **120**, 2763-2773.
11. A. Serge, N. Bertaux, H. Rigneault and D. Marguet, *Nat. Methods*, 2008, **5**, 687-694.
12. S. Saffarian, Y. Li, E. L. Elson and L. J. Pike, *Biophy J.*, 2007, **93**, 1021-1031.
13. A. Abulrob, Z. Lu, E. Baumann, D. Vobornik, R. Taylor, D. Stanimirovic and L. J. Johnston, *J. Biol. Chem.*, 2010, **285**, 3145-3156.
14. T. W. J. Gadella and T. M. Jovin, *J. Cell Biol.*, 1995, **129**, 1543-1558.
15. M. Zhou, S. Felder, M. Rubinstein, D. R. Hurwitz, A. Ullrich, I. Lax and J. Schlessinger, *Biochemistry*, 1993, **32**, 8193-8198.
16. G. Binnig, C. F. Quate and C. Gerber, *Phys. Rev. Lett.*, 1986, **56**, 930-933.
17. D. J. Muller, *Biochemistry*, 2008, **47**, 7986-7998.

18. J. Song, J.-M. Arbona, Z. Zhang, L. Liu, E. Xie, J. Elezgaray, J.-P. Aime, K. V. Gothelf, F. Besenbacher and M. Dong, *J. Am. Chem. Soc.*, 2012, **134**, 9844-9847.

19. A. Gillis, V. Dupres, G. Delestrait, J. Mahillon and Y. F. Dufrene, *Nanoscale*, 2012, **4**, 1585-1591.

20. M. Cai, W. Zhao, X. Shang, J. Jiang, H. Ji, Z. Tang and H. Wang, *Small*, 2012, **8**, 1243-1250.

21. H. J. Butt, B. Cappella and M. Kappl, *Surf. Sci. Rep.*, 2005, **59**, 1-152.

22. P. Hinterdorfer and Y. F. Dufrene, *Nat. Methods*, 2006, **3**, 347-355.

23. Y. P. Shan, J. F. Huang, J. J. Tan, G. Gao, S. H. Liu, H. D. Wang and Y. X. Chen, *Nanoscale*, 2012, **4**, 1283-1286.

24. X. Hao, N. Zhu, T. Gschneidtner, E. O. Jonsson, J. Zhang, K. Moth-Poulsen, H. Wang, K. S. Thygesen, K. W. Jacobsen, J. Ulstrup and Q. Chi, *Nat. Commun.*, 2013, **4**.

25. C. Stroh, H. Wang, R. Bash, B. Ashcroft, J. Nelson, H. Gruber, D. Lohr, S. M. Lindsay and P. Hinterdorfer, *Proc. Natl. Acad. Sci. U. S. A.*, 2004, **101**, 12503-12507.

26. H. Wang, Y. Dalal, S. Henikoff and S. Lindsay, *Epigenetics Chromatin*, 2008, **1**.

27. J. G. Jiang, X. Hao, M. J. Cai, Y. P. Shan, X. Shang, Z. Y. Tang and H. D. Wang, *Nano Lett.*, 2009, **9**, 4489-4493.

28. H. Wang, L. Obenauer-Kutner, M. Lin, Y. Huang, M. J. Grace and S. M. Lindsay, *J. Am. Chem. Soc.*, 2008, **130**, 8154-8155.

29. D. Lohr, R. Bash, H. Wang, J. Yodh and S. Lindsay, *Methods*, 2007, **41**, 333-341.

30. A. Ebner, L. Wildling, A. S. Kamruzzahan, C. Rankl, J. Wruss, C. D. Hahn, M. Holzl, R. Zhu, F. Kienberger, D. Blaas, P. Hinterdorfer and H. J. Gruber, *Bioconjug. Chem.*, 2007, **18**, 1176-1184.

31. Y. Wang, J. Gao, X. Guo, T. Tong, X. Shi, L. Li, M. Qi, Y. Wang, M. Cai, J. Jiang, C. Xu, H. Ji and H. Wang, *Cell research*, **2014**, doi: 10.1038/cr.2014.89.

32. E. G. Hofman, M. O. Ruonala, A. N. Bader, D. van den Heuvel, J. Voortman, R. C. Roovers, A. J. Verkleij, H. C. Gerritsen and P. M. van Bergen En Henegouwen, *J. Cell Sci.*, 2008, **121**, 2519-2528.

33. E. Evans, *Faraday Discuss.*, 1998, **111**, 1-16.

34. E. Evans and K. Ritchie, *Biophys. J.*, 1997, **72**, 1541-1555.

35. P. Hinterdorfer, H. J. Gruber, F. Kienberger, G. Kada, C. Riener, C. Borken and H. Schindler, *Colloid. Surface. B.*, 2002, **23**, 115-123.

36. W. Zhao, S. Liu, M. Cai, H. Xu, J. Jiang and H. Wang, *Chem. Commun.*, 2013, **49**, 2980-2982.